Enhanced external counterpulsation improves peripheral artery function and glucose tolerance in subjects with abnormal glucose tolerance

J. S. Martin, D. T. Beck, J. M. Aranda, Jr. and R. W. Braith

J Appl Physiol 112:868-876, 2012. First published 22 December 2011;
doi:10.1152/japplphysiol.01336.2011

Journal of Applied Physiology publishes original papers that deal with diverse areas of research in applied physiology, especially those papers emphasizing adaptive and integrative mechanisms. It is published 12 times a year (monthly) by the American Physiological Society, 9650 Rockville Pike, Bethesda MD 20814-3991. ISSN: 0363-6143, ESSN: 1522-1563. Visit our website at http://www.the-aps.org/.

J Appl Physiol 112: 868–876, 2012.
First published December 22, 2011; doi:10.1152/japplphysiol.01336.2011.

Enhanced external counterpulsation improves peripheral artery function and glucose tolerance in subjects with abnormal glucose tolerance

J. S. Martin,[1] D. T. Beck,[1] J. M. Aranda, Jr.,[2] and R. W. Braith[1]

[1]*Department of Applied Physiology and Kinesiology, College of Health and Human Performance, and* [2]*Division of Cardiovascular Medicine, College of Medicine, University of Florida, Gainesville, Florida*

Submitted 27 October 2011; accepted in final form 19 December 2011

Martin JS, Beck DT, Aranda JM Jr., Braith RW. Enhanced external counterpulsation improves peripheral artery function and glucose tolerance in subjects with abnormal glucose tolerance. *J Appl Physiol* 112: 868–876, 2012. First published December 22, 2011; doi:10.1152/japplphysiol.01336.2011.—*Background:* in coronary artery disease patients, enhanced external counterpulsation (EECP) improves peripheral arterial function and nitric oxide (NO) bioavailability, which have been implicated in the pathogenesis of abnormal glucose tolerance (AGT). We sought to evaluate the effects of EECP on outcomes of arterial function, glucose tolerance, and skeletal muscle morphology in subjects with AGT. *Methods and Results:* 18 subjects with AGT were randomly (2:1 ratio) assigned to receive either 7 wk (35 1-h sessions) of EECP ($n = 12$) or 7 wk of standard care (control; $n = 6$). Peripheral vascular function, biochemical assays, glucose tolerance, and skeletal muscle morphology were evaluated before and after EECP or control. EECP increased normalized brachial artery (27%) and popliteal artery (52%) flow-mediated dilation. Plasma nitrite/nitrate (NOx) increased (30%) and 8-isoprostane-PGF-$F_{2\alpha}$, a marker of lipid peroxidation in the plasma, decreased (−23%). Fasting plasma glucose declined (−16.9 ± 5.4 mg/dl), and the homeostasis model assessment of insulin resistance (HOMA-IR) decreased (31%) following EECP. Plasma glucose 120 min after initiation of oral glucose tolerance testing decreased (−28.3 ± 7.3 mg/dl), and the whole body composite insulin sensitivity index (C-ISI) increased (21%). VEGF concentrations increased (75%), and vastus lateralis skeletal muscle biopsies demonstrated improvements in capillary density following EECP. No change was observed in cellular signaling pathways, but there was a significant increase GLUT-4 protein expression (47%) following EECP. *Conclusions*: our findings provide novel evidence that EECP has a beneficial effect on peripheral arterial function and glucose tolerance in subjects with AGT.

vascular function; glycemic control; diabetes; capillary density

ABNORMAL GLUCOSE TOLERANCE (AGT), observed in individuals classified as prediabetic or having type II diabetes mellitus (T2D), is characterized by elevated postprandial plasma glucose concentrations secondary to the marked decline in insulin-mediated glucose transport in skeletal muscle and adipose tissue (i.e., insulin resistance). The Centers for Disease Control estimated that in 2010, among people aged ≥20 yr in the United States, 25.6 million had diabetes and another 79 million were prediabetic (8). Among the estimated 25.6 people in United States with diabetes, ~90–95% of those have T2D (8). Because skeletal muscle accounts for over two-thirds of the clearance of a hyperglycemic challenge (18), interventions that increase skeletal muscle glucose uptake are known to improve glucose homeostasis in patients with prediabetes (17) and T2D (12). Treatment and management of AGT can range from alteration of diet and physical activity habits to pharmacotherapy. However, compliance with exercise (~25%)(2) and drug therapy (36–93%)(10) in people with T2D is low. Consequently, alternative methods that improve glucose homeostasis for the prevention and treatment of T2D should be considered.

Glucose uptake in skeletal muscle cells is regulated by three known pathways: *1*) insulin-mediated cell signaling; *2*) contraction-mediated cell signaling; and *3*) nitric oxide (NO)-mediated cell signaling. Insulin-mediated glucose uptake, which is impaired with AGT, and contraction-mediated glucose uptake (preserved in AGT) have been well characterized. The NO-mediated pathway increases glucose uptake through a mechanism that is distinct from these pathways. NO donors significantly increase skeletal muscle glucose uptake in the presence of wortmannin, a PI3K inhibitor, indicating that the NO signaling pathway is distinct from the insulin/PI3K-dependent mechanism (16). Furthermore, although the contraction- and NO-mediated glucose uptake pathways overlap downstream of AMPK, L-NAME, a nitric oxide synthase inhibitor, does not abolish contraction-mediated glucose uptake and NO donors have an additive effect on glucose uptake in contracting isolated skeletal muscle (16). NO has been shown to increase GLUT-4 protein expression (22) and GLUT-4 translocation to the cell membrane via a cyclic guanosine monophosphate (cGMP) and AMPK-dependent mechanism (16). Importantly, Solomon et al. (33) recently showed that increasing severity of glucose intolerance was associated with progressive declines in plasma NOx concentrations, capillary density, capillaries per fiber, and the number of capillary contacts per muscle fiber. Therefore, therapies that target not only NO bioavailability, but also capillary density, may be effective treatment strategies for AGT.

EECP is a noninvasive FDA approved therapy that reduces angina episodes and nitrate usage in patients with coronary artery disease (CAD) who experience refractory angina despite aggressive pharmacotherapy and revascularization (3, 36). EECP involves sequential inflation (~300 mmHg) during cardiac diastole of three pneumatic EECP cuffs from the calves to buttocks. The compressive cuffs create blood flow patterns in the femoral (retrograde) and brachial (antegrade) arteries that acutely increase shear rate (40). Previously, we and others demonstrated that external compression upregulates NO bioavailability and improves endothelial-dependent flow-mediated dilation (FMD) in muscular conduit arteries (5, 24).

The possible clinical benefits of EECP in subjects with AGT are unknown. We hypothesized that EECP treatment would elicit changes in arterial function and NO bioavailability in subjects with non-insulin dependent AGT similar to those observed in CAD patients. We further hypothesized that EECP

Address for reprint requests and other correspondence: J. S. Martin, Dept. of Biomedical Sciences, Univ. of Missouri-Columbia, W108 Vet. Med. Bldg., 1600 E. Rollins, Columbia, MO 65211 (e-mail: martinjs@missouri.edu).

treatment would improve measures of fasting glucose and insulin concentrations and glucose tolerance. To test our hypothesis we examined potential mechanisms for proposed improvement in glycemic control and glucose tolerance, including cellular signaling, skeletal muscle protein expression, and capillary density.

METHODS

Subjects. Eighteen ($n = 18$) subjects with non-insulin dependent AGT were recruited from the local community by advertisement. AGT was defined as the presence a plasma glucose concentration of >140 mg/d. after a 2-h oral glucose tolerance test as determined through screening. Subjects were randomized in a 2:1 manner into either an EECP treatment group or a control group. Unequal randomization was used to improve the precision of the treatment effect. This design requires more subjects to achieve the same power as would be necessary with a 1:1 randomization and therefore does not bias the study. Laboratory testing was performed at study entry and after 35 1-h EECP sessions (7 wk) or matched control period. The study was approved by the University of Florida Health Science Center Institutional Review Board, and written informed consent was obtained from all participants.

Exclusion criteria. Exclusion criteria were insulin dependence for glycemic control; any major illness in the prior 3 mo; previous treatment with EECP; participation in moderate intensity exercise for 20 min, two or more times per week; history of deep vein thrombosis, phlebitis, stasis ulcer, and/or pulmonary embolism; aged less than 21 yr or greater than 75 yr; uncontrolled hypertension (defined as a systolic blood pressure of 180 mmHg or more and/or a diastolic blood pressure of 110 mmHg or more, measured as the average of at least two readings, obtained at different occasions); systemic hypotension; cardiac arrhythmia that would significantly interfere with the triggering of the EECP device; and acute coronary syndrome such as unstable angina or acute myocardial infarction.

EECP and control groups. Subjects in the EECP group ($n = 12$) received 35 1-h daily sessions of EECP for seven consecutive weeks with target inflation pressures of 300 mmHg per cuff. Subjects in the control group ($n = 6$) received continued medical care with no EECP intervention.

Body composition. Height and weight were measured using standard procedures. Whole body and regional adiposity were determined using dual-energy x-ray absorptiometry (Lunar, Madison, WI).

Peripheral FMD. The FMD technique was used to determine endothelial-dependent reactivity in the brachial and popliteal arteries. At study entry and within 24–48 h after the final EECP therapy treatment or time-matched control, subjects fasted for at least 8 h and withheld all vasoactive medications for 10–12 h. After lying quietly for 15 min, a 10.5-MHz linear phase array ultrasound transducer (ATL HDI 3000; Advanced Technologies) was used to image the right brachial artery longitudinally. Resting baseline end-diastolic brachial diameters and blood velocity were obtained with the transducer placed 3–5 cm above the anticubital fossa. After obtaining baseline diameter measures, reactive hyperemia was produced by inflating a blood pressure cuff placed on the upper forearm, 1–2 cm below the elbow, for 5 min at 200 mmHg. The transducer was manually held in the same position for the duration of cuff inflation. Immediately following cuff release, brachial artery blood flow velocity was measured for 20 s. Brachial artery diameter was then imaged and recorded for an additional 2 min. Ultrasound images were recorded directly to a digital storage device via video interface (Pinnacle, Avid Technology) for off-line electronic image analysis using automated FMD software (Vascular Research Tools; Medical Imaging Applications).

Brachial artery diameters were determined during end-diastole (gated with electrocardiogram R wave) by measuring the distance between the near and far wall of the intima. Brachial FMD was calculated in absolute (mm) and relative (FMD%) peak change in brachial artery diameter in response to the hyperemic stimulus. Brachial measurements were normalized to the mean shear rate calculated from the first 10 s following cuff release. With the use of artery diameter and mean velocity Doppler measurements, blood flow in the brachial artery was calculated using the following equation: blood flow (ml/min) = mean velocity·π·(diameter/2)^2·60. Additionally, in the absence of blood viscosity, shear rate is measured by the following equation: shear rate (s^{-1}) = 4·mean blood velocity (cm/s)·diameter (cm^{-1}).

Popliteal artery FMD was performed at the popliteal fossa, 2 to 3 cm above the bifurcation, with subjects in the prone positions. The approximate FMD protocol described above for brachial FMD was also used for popliteal artery FMD.

Blood collection and biochemical assays. Venipuncture was performed before and after 35 sessions of EECP or time-matched control period. Measurement of the stable NO metabolites nitrite and nitrate (NOx) were used to estimate NO production. Subjects kept a diet diary and followed the National Institutes of Health low-nitrate diet guidelines a minimum of 48 h before each blood draw (30). NOx and 6-keto-prostaglandin $F_{1\alpha}$ (6-keto-$PGF_{1\alpha}$), the major metabolite of prostacyclin, were measured by commercial assays (Cayman, Ann Arbor, MI). Enzyme-linked immunosorbent assay kits were also used to measure plasma levels of endothelin-1 (ET-1) (Quantikine, Minneapolis, MN), 8-iso-prostaglandin $F_{2\alpha}$ (8-iso-$PGF_{2\alpha}$; Assay Designs, Ann Arbor, MI), vascular endothelial growth factor (VEGF; Quantikine), asymmetric dimethylarginine (ADMA) (Alpco, Salem, NH), and insulin (Alpco). Plasma glucose was measured using an automated glucose oxidase assay (YSI 2300 StatPlus; YSI, Yellow Springs, OH). The intra-assay coefficients of variation were 3.2% for NOx, 5.5% for 6-keto-$PGF_{1\alpha}$, 3.4% for ET-1, 1.3% for 8-iso-$PGF_{2\alpha}$, 6.7% for VEGF, 5.3% for ADMA, and 10.3% for insulin.

Glucose tolerance. Oral glucose tolerance tests (OGTT) were performed in all subjects at study entry and at 24–48 h after 35 1-h sessions of EECP or time-matched control period. During the 3 days prior to each OGTT, subjects were instructed to consume a standardized diet, consisting of at least 200 g of carbohydrate per day, while abstaining from caffeine and alcohol. Subjects reported to the laboratory in the morning following an overnight fast and withheld vasoactive medications for 10–12 h and glycemic control medications for at least 24 h. A catheter was placed in a vein in the anticubital space and, baseline blood samples were drawn at −10, −5, and 0 min to account for the pulsatile nature of insulin secretion. An average of the three baseline time points was used to determine fasting plasma insulin (FPI) and fasting plasma glucose (FPG) concentrations. Following ingestion of a glucose beverage (Fisherbrand Glucose Tolerance Test Beverage, 7.5 g glucose/fl oz., 10 oz. beverage, 75 g of glucose ingested), blood samples were taken at 30, 60, 90, and 120 min from the time the drink was finished. Subjects were instructed to drink the entire beverage as quickly as possible and in a time not to exceed 3 min.

Resting measures of FPG and FPI were also used to calculate the homeostatic model assessment of insulin resistance (HOMA-IR) as follows: [FPG (mg/dl)·FPI (μIU/ml)]/405. Plasma glucose and insulin values at 0, 30, 60, 90, and 120 min of OGTT were used to calculate the whole body insulin sensitivity index (C-ISI) as follows: $\sqrt{}$[(FPG·FPI)·(mean plasma glucose·mean plasma insulin)] (24).

Muscle processing. Skeletal muscle biopsies were obtained from all subjects before and 36–48 h following 35 1-h sessions of EECP. Skeletal muscle tissue (~150 mg) was extracted from the right vastus lateralis of each subject using a percutaneous needle under local subcutaneous anesthetic (1% lidocaine) using a modification of the Bergstrom technique (6, 14). Connective tissue and adipose deposits were removed from the muscle biopsy samples, and two-thirds (~100 mg) of the sample was immediately snap frozen in liquid nitrogen and stored at −80°C for quantitative protein analysis via Western blotting. The other one-third of the muscle biopsy sample (~50 mg) was

separated for cryosectioning. After ensuring alignment of muscle fibers at resting length, this portion was frozen in optimal cutting temperature (OCT) medium by liquid nitrogen-cooled isopentane and stored at −80°C until cryosectioning.

Western blotting. Frozen muscle samples were homogenized using procedures as reported by Sakamoto et al. (32). Protein concentrations were measured using the DC Protein Assay Kit (Bio-Rad, 500–0116). Aliquots of muscle homogenate (50 μg) were separated in 4–20% SDS-PAGE gels, transferred to nitrocellulose membranes, and stained with Ponceau S to verify transfer. Separate protein blots were probed for proteins of interest along with β-actin as a loading control. Blots were blocked with Odyssey blocking buffer (LI-COR Biosciences) before incubation with primary and secondary antibodies. The primary antibodies used were: goat anti-$Akt_{1/2}$ (N-19) (Santa Cruz Biotechnology; sc-1619), rabbit anti-phospho-$AKT_{1/2/3}$ (Ser473) (Santa Cruz Biotechnology; sc-7985-R), mouse anti-$AMPK_{\alpha}$ (Cell Signaling Technology; 2793), rabbit anti-phospho(Thr172)-$AMPK_{\alpha 2}$ (Millipore; 07–681), rabbit anti-TBC1D4 (Abcam; ab24469), rabbit anti-phospho (Thr642)-TBC1D4 (Novus Biologicals; NBP1–44074), goat anti-GLUT-4 (Santa Cruz Biotechnology; sc-1608), and rabbit anti-β-actin (Abcam; ab8227). Incubations with the secondary antibodies IRDye 680CW donkey anit-goat, 680CW donkey anti-mouse, 800CW donkey anti-mouse, and 800CW donkey anti-rabbit (LI-COR Biosciences) were performed. Protein blots were scanned, and proteins of interest were detected using the Odyssey infrared imaging system (LI-COR Biotechnology, Lincoln, NE).

Muscle capillarization. Frozen sections of muscle biopsy tissue were cut (10 μm) in a cryostat and fixed on poly-L-lysine-coated glass slides. Slides were fixed in Carnoy's fixative (60% ethyl alcohol, 30% chloroform, and 10% glacial acetic acid), and capillaries were identified using a periodic acid-Schiff stain after pretreatment with amylase, described by Andersen (1). Images of the muscle sections were captured with an inverted microscope (Olympus America; Center Valley, PA). Stained sections were analyzed by magnifying and projecting numerous artifact-free sections of ~0.20 mm^2 areas onto a screen. Number of fibers and capillaries was determined on 166 ± 13 fibers per biopsy. Areas were assessed by manual drawing of the perimeter using the National Institutes of Health's public software (Image J, NIH).

Statistical analysis. This study was designed as an open label, unbalanced, randomized study of EECP vs. standard of care for subjects with AGT. All data were tested for normal distribution using the Shapiro-Wilk test for normality. An alpha level of $P \leq 0.05$ was required for statistical significance. Satterthwaite corrected two sample *t*-tests of baseline subject characteristics were performed to determine differences between groups at baseline. A repeated-measures two-way analysis of variance was used to evaluate the continuous primary dependent variables associated with FMD, humoral markers, capillarity, fasting indexes of glycemic control, and dynamic measures of glucose tolerance. When a significant group-by-time interaction was observed, within-group paired *t*-tests were performed to analyze differences between time points. Furthermore, between-group comparisons at each time point were performed using a Satterthwaite corrected two sample *t*-test with Bonferroni correction for pairwise comparison. To achieve an overall family error rate of 5% for two between-group comparisons (EECP post vs. control baseline and post), α was adjusted two comparisons, 0.05/2 = 0.025. Western blot proteins of interest were analyzed using the Satterthwaite corrected two sample *t*-test of percent change from baseline as the dependent variable and study group (EECP vs. control) as the independent variable. Pearson correlations were performed to compare magnitude of change in variables with an alpha level of $P < 0.05$ for two-tailed analysis. All statistical analyses were performed using IBM SPSS Statistics 19 for Windows (Chicago, IL). All data are reported as mean ± SE.

RESULTS

All subjects completed the entire EECP therapy protocol or time-matched control period without adverse events. Table 1 contains the subject descriptive characteristics and metabolic profile. There were no differences between the two groups at study entry with respect to age, body mass index (BMI), percent body fat, trunk-to-limb fat mass ratio, resting heart rate, blood pressure, FPG, FPI, HOMA-IR, plasma glucose 120 min after initiation of an OGTT (PPG_{120}), and the C-ISI. One of six subjects (17%) in the control group and four of twelve (33%) subjects in the EECP group had prediabetes. The remaining subjects had overt T2D. There was no significant difference between the groups in diabetic status at study entry ($P = 0.486$). Table 2 contains the subject drug therapy regimens at study entry. There were no significant differences between groups with respect to pharmacologic therapies at study entry. No significant interactions with pharmacotherapy or diabetic status were observed with primary outcomes. Med-

Table 1. *Subject descriptive characteristics and metabolic profile*

	EECP (n = 12)		Control (n = 6)		Within EECP
	Before	After	Before	After	P Value
Age, yr	64.31 ± 1.95	64.45 ± 1.95	64.00 ± 2.76	64.17 ± 2.76	
Height, cm	178.7 ± 1.8	178.7 ± 1.8	179.1 ± 2.5	178.9 ± 2.5	0.999
Body weight, kg	97.2 ± 5.0	96.8 ± 4.9	99.2 ± 7.1	99.1 ± 6.9	0.351
Body mass index, kg/m^2	30.33 ± 1.26	30.23 ± 1.20	29.49 ± 1.78	29.67 ± 1.69	0.484
Body fat, %	32.05 ± 1.71	31.87 ± 1.60	32.67 ± 2.42	32.28 ± 2.27	0.408
Trunk/limb fat mass	1.61 ± 0.14	1.64 ± 0.15	1.73 ± 0.19	1.84 ± 0.21	0.405
Resting HR, beats/min	65 ± 6.9	63 ± 7.0	65 ± 13.2	66 ± 14.0	0.328
Resting SBP, mmHg	139 ± 4.6	129 ± 4.6*	143 ± 6.5	142 ± 6.5	0.003
Resting DBP, mmHg	81 ± 2.7	80 ± 2.6	83 ± 3.8	83 ± 3.7	0.372
FPG, mg/dl	143.9 ± 8.5	127.0 ± 6.6*	138.3 ± 12.0	140.2 ± 9.4	0.011
FPI, μIU/ml	10.52 ± 1.45	8.72 ± 1.21	9.71 ± 1.96	9.87 ± 1.63	0.108
HOMA-IR, A.U.	3.62 ± 1.87	2.63 ± 1.33*	3.25 ± 0.58	3.38 ± 0.89	0.008
PPG_{120}, mg/dl	224.4 ± 24.6	196.1 ± 24.7*	246.0 ± 34.8	249.4 ± 34.9	0.003
C-ISI, A.U.	2.77 ± 0.40	3.35 ± 0.42*	2.69 ± 0.57	2.50 ± 0.59	0.023

Data are presented as means ± SE. HR, heart rate; SBP, systolic blood pressure; DBP, diastolic blood pressure; FPG, fasting plasma glucose; FPI, fasting plasma insulin; HOMA-IR, homeostatic model assessment-insulin resistance; PPG_{120}, postprandial glucose at 120 min; C-ISI, composite insulin sensitivity index. There were no significant differences in descriptive characteristics or metabolic profile between enhanced external counterpulsation (EECP) and control groups at baseline. Significance was determined from post hoc within groups paired *t*-tests when a significant group-by-time interaction ($P < 0.05$) was observed from repeated measures ANOVA. *$P < 0.05$.

Table 2. *Subject drug regimens*

	EECP (n = 12)	Control (n = 6)	Between Groups P Value
Thiazolidinedione therapy	3 (25)	1 (17)	0.709
Sulfonylurea therapy	2 (17)	1 (17)	0.999
Lipid-lowering therapy	7 (58)	3 (50)	0.755
β-blocker therapy	2 (17)	1 (17)	0.990
CCB therapy	3 (25)	1 (17)	0.709
ACE inhibitor/ARB therapy	3 (25)	2 (33)	0.729
Diuretic therapy	3 (25)	1 (17)	0.709

Data are expressed as the number of subjects per group and the percentage (in parentheses). CCB, calcium channel blocker; ACE, angiotensin converting enzyme; ARB, angiotensin receptor blocker. There were no significant differences ($P > 0.05$) between EECP and control groups in drug regimens.

ications were not altered during the study period, and all subjects were informed to abstain from initiating any changes in physical activity and dietary habits, except as noted in the methods for measurements.

EECP decreased peripheral blood pressure. No changes were observed in resting heart rates between groups or within groups after 35 sessions of EECP therapy or 7 wk of matched control. Peripheral systolic blood pressure did not differ between groups at study entry. There was a significant decrease in peripheral systolic blood pressure following EECP therapy (-10.0 ± 2.7 mmHg, $P < 0.01$), but no change in the control group (-0.3 ± 3.3 mmHg, $P = 0.94$). No changes were observed in peripheral diastolic blood pressure in either group (-1.0 ± 1.1 and -0.3 ± 1.7 mmHg, EECP and control, respectively). These changes in peripheral systolic blood pressure are similar those observed in CAD patients following EECP (5).

EECP improved brachial and popliteal FMD. The results of flow-mediated dilation studies of the brachial and popliteal arteries following EECP or control are contained in Table 3. At study entry, resting diameter and FMD did not differ between groups for the brachial and popliteal arteries. EECP therapy improved absolute brachial artery FMD, percent change in dilation, and FMD normalized to shear rate in the first 10 s after cuff release. EECP also improved popliteal FMD normalized during the first 10 s after cuff release; however, improvements in absolute popliteal artery FMD and percent change in dilation did not reach statistical significance. No changes in brachial or popliteal artery FMD occurred in the control group.

EECP increased plasma NOx and 6-keto-PGF$_{1\alpha}$. Plasma levels of NOx, 6-keto-PGF$_{1\alpha}$, and ET-1 did not differ between groups at study entry. EECP increased plasma NOx (Fig. 1*A*) and 6-keto-PGF$_{1\alpha}$ (Fig. 1*B*). Furthermore, plasma concentrations of NOx following 7 wk of EECP therapy were significantly greater than the control group following matched control period ($P < 0.025$). No changes in plasma NOx and 6-keto-PGF$_{1\alpha}$ were observed in the control group. There was no significant change in plasma ET-1 (Fig. 1*C*) or the NOx/ET-1 ratio in either group.

EECP improved redox balance. At study entry, plasma levels of 8-iso-PGF$_{2\alpha}$ and ADMA did not differ between groups. Following EECP therapy, there was a significant decrease in plasma levels of 8-iso-PGF$_{2\alpha}$, but no significant change in the control group (Fig. 2*A*). There was also a significant decrease in plasma levels of ADMA in the EECP group following 35 sessions and no significant change in the control group (Fig. 2*B*). Furthermore, plasma concentrations of ADMA following EECP were significantly less than the control group at the same time-point ($P < 0.025$).

EECP improved fasting markers of glycemic control. Baseline and post values for FPG, FPI, and the HOMA-IR are presented in Table 1. There were no differences between groups at study entry. There was a significant decrease in FPG

Table 3. *Brachial and popliteal artery flow-mediated dilation characteristics*

	EECP (n = 12)		Control (n = 6)	
	Before	After	Before	After
Brachial artery				
Resting diameter, mm	4.50 ± 0.15	4.55 ± 0.13	4.33 ± 0.21	4.27 ± 0.18
Mean blood velocity, cm/s				
Resting	3.52 ± 0.55	3.31 ± 0.54	3.46 ± 0.78	4.04 ± 0.77
Hyperemia	22.3 ± 1.7	23.4 ± 1.3	23.9 ± 2.4	24.3 ± 1.9
Mean shear rate, s^{-1}				
Resting	32.0 ± 4.9	29.4 ± 4.7	31.9 ± 6.9	38.1 ± 6.6
Hyperemia	241 ± 19	258 ± 17	270 ± 27	272 ± 24
Absolute FMD, mm	13.0 ± 1.1	18.2 ± 2.0*	13.9 ± 1.5	13.4 ± 2.7
FMD, %	2.90 ± 0.30	4.01 ± 0.50*	3.22 ± 0.42	3.16 ± 0.70
Normalized FMD, s^{-1}	0.015 ± 0.20	0.020 ± 0.002*	0.016 ± 0.003	0.015 ± 0.003
Popliteal Artery				
Resting diameter, mm	6.28 ± 0.34	6.25 ± 0.36	6.49 ± 0.49	6.39 ± 0.51
Mean blood velocity, cm/s				
Resting	1.33 ± 0.22	1.38 ± 0.16	1.34 ± 0.31	1.54 ± 0.23
Hyperemia	10.6 ± 1.6	12.3 ± 1.3	12.8 ± 2.4	14.1 ± 1.9
Mean shear rate, s^{-1}				
Resting	9.0 ± 1.5	9.5 ± 1.3	8.3 ± 2.1	9.8 ± 1.9
Hyperemia	71.8 ± 15.4	79.1 ± 10.1	75.9 ± 23.1	85.8 ± 15.1
Absolute FMD, mm	9.3 ± 0.9	15.4 ± 1.9	11.6 ± 1.3	13.3 ± 2.6
FMD, %	1.50 ± 0.14	2.43 ± 0.21	1.73 ± 0.21	1.92 ± 0.34
Normalized FMD, s^{-1}	0.023 ± 0.003	0.035 ± 0.004*	0.026 ± 0.005	0.026 ± 0.006

Data are expressed as means ± SE. Mean blood velocity, blood flow, and shear rate were measured at baseline and during the first 10 s following cuff release; FMD, flow-mediated dilation expressed as absolute dilation (mm), relative dilation to baseline (%), and dilation normalized to mean hyperemic shear rate (s^{-1}). *$P < 0.05$ within-EECP group.

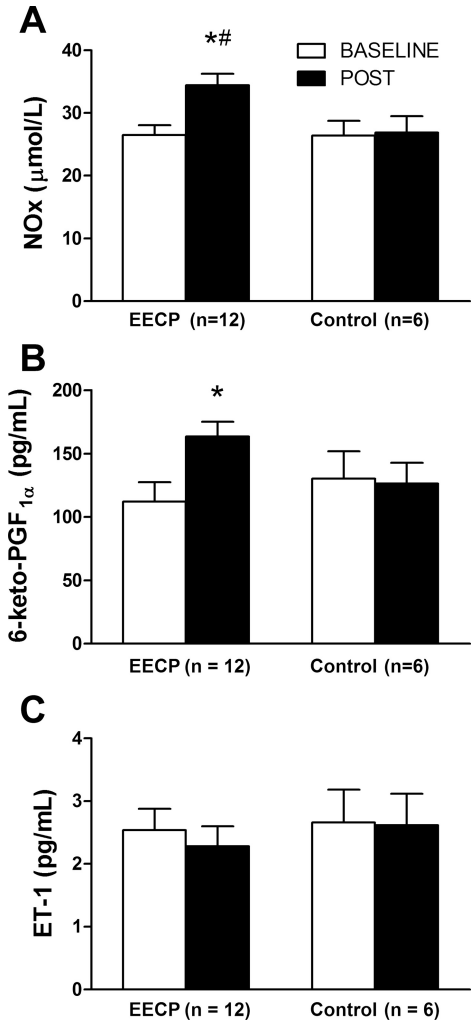

Fig. 1. Data are absolute values before (BASELINE) and after (POST) enhanced external counterpulsation (EECP) or 7 wk of control. When significant interactions were determined by repeated-measures ANOVA, within-group differences were determined by paired *t*-tests. Between groups comparisons were evaluated using a Satterthwaite correct *t*-test with Bonferonni correction for multiple comparisons. *A*: plasma concentrations of nitrite/nitrate (NOx; μmol/l); *B*: plasma concentrations of 6-keto-prostaglandin $F_{1\alpha}$ (6-keto-$PGF_{1\alpha}$; pg/ml); and *C*: plasma concentrations of endothelin-1 (ET-1; pg/ml). $*P < 0.05$ vs. BASELINE within groups; $\#P < 0.025$ vs. control group at same time point. Data are expressed as means ± SE.

in the EECP group, but no significant change in the control group. FPI did not change in either the EECP or control group. The HOMA-IR was significantly decreased following EECP therapy but did not change significantly in the control group.

EECP improved dynamic indexes of oral glucose tolerance. PPG_{120} and C-ISI at baseline and after EECP or control are presented in Table 1. There was a significant decrease in PPG_{120} in the EECP group following 35 sessions but did not change significantly in the control group. The C-ISI significantly increased following EECP therapy but did not change in the control group.

EECP increased markers of angiogenesis/vasculogenesis. At study entry, plasma levels of VEGF did not differ between groups. In addition, there was no difference between groups in baseline fiber cross-sectional surface area (FSA), capillary to fiber ratios (C/F), the number of capillaries per square millimeter of surface area (CD), and the ratio of the number of capillary contacts per fiber (CC/F). EECP therapy increased VEGF (9.74 ± 1.59 to 17.04 ± 2.65 pg/ml and 9.94 ± 2.24 to 8.99 ± 3.75 mg/dl in EECP vs. control, respectively; $P < 0.05$). Table 4 contains the results from immunostaining for capillary density in vastus lateralis skeletal muscle before and after EECP therapy or control. A representative photomicrograph can be seen in Fig. 3. The C/F ratio and CD were significantly increased with EECP therapy. Furthermore, there was a trend for an increase in CC/F with EECP therapy, however, the group×time effect did not reach statistical significance ($P < 0.10$). No changes were observed in C/F ratio, CD, and CC/F in the control group. No change was observed in FSA in either group.

Effects of EECP on protein expression in vastus lateralis skeletal muscle biopsy homogenate. To assess phosphorylation state of Akt, AMPK, and TBC1D4, phosphorylated protein is expressed relative to total protein as a ratio. All other protein expression was normalized to β-actin loading control. p-$Akt_{1/2/3}$/total Akt1/2, p-$AMPK_{\alpha 2}$/total $AMPK_{\alpha}$, and p-TBC1D4/total TBC1D4 did not change in either group (Fig. 4, *A*, *B*, and *C*, respectively). There was a significant increase in expression of GLUT-4 in the EECP group but no change in GLUT-4 expression in the control group (Fig. 4*D*).

DISCUSSION

To our knowledge, this is the first study to evaluate the effects of EECP on arterial function, fasting glucose and

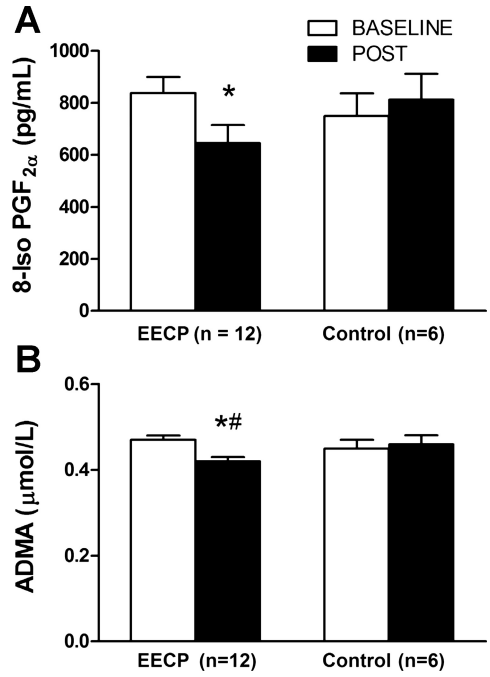

Fig. 2. Data are absolute values before (BASELINE) and after (POST) EECP or 7 wk of control. When significant interactions were determined by repeated-measures ANOVA, within-group differences were determined by paired *t*-tests. Between groups comparisons were evaluated using a Satterthwaite correct *t*-test with Bonferonni correction for multiple comparisons. *A*: plasma concentrations of 8-iso-prostaglandin-$F_{2\alpha}$ (8-iso-$PGF_{2\alpha}$; pg/ml); *B*: plasma concentrations of asymmetric dimethylarginine (ADMA; μmol/l). $*P < 0.05$ vs. BASELINE within groups; $\#P < 0.025$ vs. control group at same time point. Data are expressed as means ± SE.

Table 4. *Skeletal muscle morphology and parameters of capillary density*

	EECP (n = 12)		Control (n = 6)		Group*Time	Within EECP
	Before	After	Before	After	P value	P value
FSA, μm^2	4719 ± 541	4720 ± 476	4076 ± 802	3852 ± 706	0.598	—
C/F ratio	1.68 ± 0.10	1.89 ± 0.07*	1.67 ± 0.15	1.59 ± 0.10	0.041	0.017
CD, mm^{-2}	454 ± 21	497 ± 19*	474 ± 26	470 ± 23	0.025	0.018
CC/F ratio	3.44 ± 0.16	3.96 ± 0.16†	3.47 ± 0.24	3.46 ± 0.23	0.067	—

Data are expressed as means ± SE. FSA,skeletal muscle fiber cross-sectional area; C/F, skeletal muscle capillary to fiber ratio; CD, capillaries per square millimeter of skeletal muscle (capillary density); CC/F, capillary contacts per fiber. *$P < 0.05$ within-EECP group; †$P < 0.10$ for repeated-measures ANOVA group*time interaction.

insulin concentrations, glucose tolerance, capillary density, and skeletal muscle protein expression in subjects with AGT. The main findings of this study are that, in subjects with AGT, EECP treatment: *1*) elicits similar changes in arterial function to those observed in coronary artery disease patients; *2*) improves fasting glucose and insulin concentrations; *3*) improves glucose tolerance; and *4*) increases capillary density and GLUT-4 protein expression in compressed skeletal muscle.

Arterial function and NO bioavailability. The distal occlusion method of assessing arterial FMD, as used in the present study, has been shown to be a valid and reliable surrogate of nitric oxide-mediated endothelial function (13). After 35 sessions of EECP treatment in subjects with AGT we observed significant improvements in brachial (27%) and popliteal (52%) artery FMD normalized to reactive hyperemic shear rate.

The mechanism responsible for the observed changes in peripheral artery FMD is likely shear stress induced by the increases in blood flow during cuff compressions. In a porcine EECP model, brachial artery blood flow velocity was shown to increase by 132% and brachial artery wall shear stress increased by >200% during lower body compression of pneumatic EECP cuffs (40). Our lab has also demonstrated that during EECP in humans, antegrade endothelial shear stress in the brachial artery was increased by 75% and retrograde endothelial shear stress in the popliteal artery was increased by 402% (15). Moreover, systolic hyperemia is likely to occur in the legs with each cuff deflation. Therefore, the robust changes in arterial blood flow and shear stress during EECP therapy may mediate changes in FMD response attributable to an increase in NO bioavailability. Indeed, the present study demonstrated that EECP resulted in a 30% increase in plasma NOx levels. Importantly, this effect has been show to persist for at least 1 mo following the culmination of 35 sessions of EECP (24).

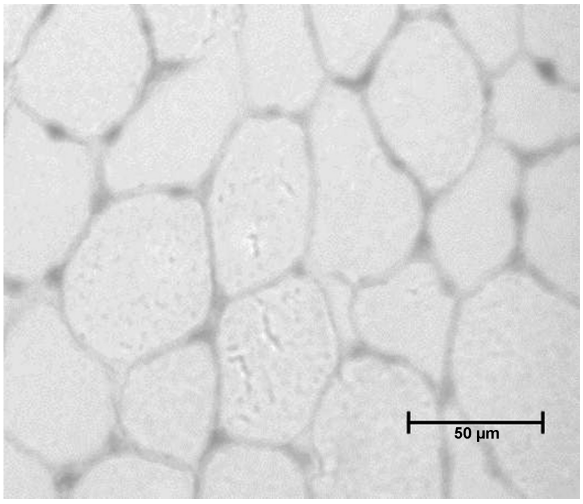

Fig. 3. Representative photomicrograph of skeletal muscle morphology. Vastus lateralis skeletal muscle biopsies were obtained and histomounts were stained using an amylase-periodic acid-Schiff base histochemical stain. Fibers and capillaries run perpendicular to the page. Bar represents 50 μm. Values of representative photomicrograph: mean fiber area = 4,825 μm^2; capillary density (CD) = 396 capillaries/mm^2; capillary to fiber ratio (C/F) = 1.79.

Oxidative stress modulates NO bioavailability and has been implicated in the development and progression of diabetes (9). Increased production of free radicals and/or impaired antioxidant defenses diminishes NO and inhibits its action (23). 8-iso-$PGF_{2\alpha}$ is suggested to be the most valid marker to assess oxidative stress in human plasma (27) and is highly correlated with glycemic control (11). The present study demonstrated that EECP resulted in a 23% decrease in 8-iso-$PGF_{2\alpha}$ after EECP treatment in subjects with AGT. This reduction is similar to that observed in CAD patients following EECP therapy(5) and potentiates greater NO bioavailability and/or glucose uptake signaling. Additionally, oxidative stress appears to be a key modulator of ADMA levels. Evidence suggests that ADMA is associated with endothelial dysfunction in a number of disorders, including AGT (35). In the present study, we are the first to demonstrate a decrease in circulating ADMA levels following EECP treatment in patients with AGT. Dimethylargininase (DDAH) activity, the major eliminator of ADMA, is also redox and shear stress sensitive (34). Although DDAH was not measured in the present study, our compelling 8-iso-$PGF_{2\alpha}$ data suggest that oxidation of DDAH may have been diminished. Second, EECP-induced shear stress could upregulate DDAH. Osani et al. (29) showed that human endothelial cells in vitro demonstrated an increase in DDAH activity at shear stress levels of ≥25 dynes/cm^2. It is plausible that DDAH activity is increased with the magnitude of shear stress invoked with EECP (~175% of baseline, 29 vs. 16 dynes/cm^2 in human brachial artery during a bout of EECP) (15).

Glycemic control and glucose tolerance. To the best of our knowledge, this is the first study to evaluate the changes in fasting glucose and insulin concentrations after EECP treatment. Following 35 sessions of EECP, subjects with AGT demonstrated marked improvements in fasting indexes of glycemic control. Fasting plasma glucose (FPG) values were decreased nearly 17 mg/dl following EECP. This 13.3% decline in FPG is similar to that observed with resistance training intervention in older men with T2D (7) and aerobic exercise

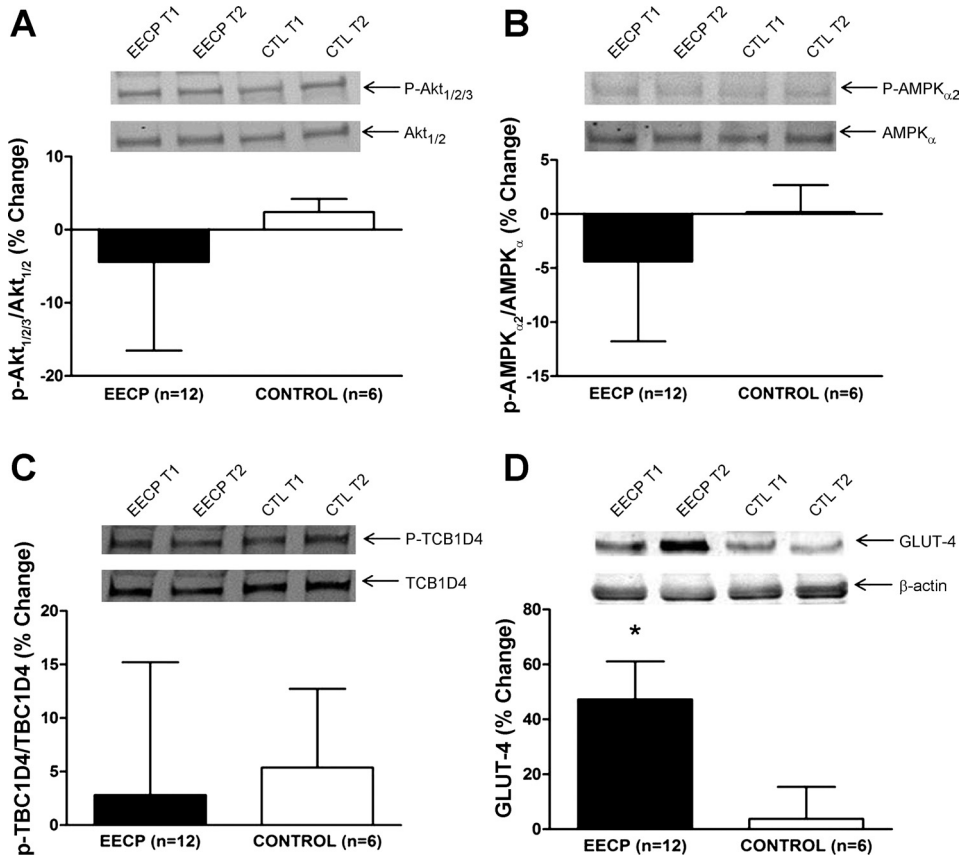

Fig. 4. Western blot analysis of skeletal muscle protein expression and phosphorylation state. Data are presented as percent change from BASELINE within group after 35 sessions of EECP or 7 wk of control (CTL). Akt, AMPK, and TBC1D4 phosphorylation states were determined by the relative optical density of phosphorylated protein to total protein. GLUT-4 expression was determined by a ratio of the optical density of GLUT-4 to β-actin. Significant differences between groups were determined using a Satterthwaite corrected *t*-test. *A*: p-$Akt_{1/2/3}$/total $Akt_{1/2}$; *B*: p-$AMPK_{\alpha 2}$/total $AMPK_{\alpha}$; *C*: p-TBC1D4/total TBC1D4; *D*: GLUT-4/β-actin. *$P < 0.05$ vs. control group. Data are expressed as means ± SE.

training older subjects with non-insulin dependent T2D and impaired glucose tolerance (37). Importantly, these changes occurred in the absence of any lifestyle modification. Moreover, subjects' weight, BMI, body fat percentage, and measures of central adiposity did not change during EECP treatment. Of particular significance, data from the Framingham Heart Study has demonstrated that for every 10 mg/dl increase in FPG there is an 18% increase in all-cause mortality (26). Further evidence for improved glycemic control following EECP in subjects with AGT is demonstrated by the 31% decline in HOMA-IR values, a marker of insulin sensitivity that correlates well with glucose disposal rates derived from hyperinsulinemic euglycemic clamp (HEC) (4).

Stronger surrogates of insulin sensitivity and glucose tolerance can be derived from the multiple sampling of plasma insulin and glucose during an OGTT. For the present study, the C-ISI developed by Matsuda et al.(25) was chosen because of high correlation with the HEC ($r = 0.73$) and validity in a wide variety of subjects with AGT (28). We observed a 21% improvement in the C-ISI after EECP treatment, and, given the strong correlation with the HEC, these results suggest improvements in glucose tolerance and insulin sensitivity. Furthermore, we observed a 28 mg/dl decrease in plasma glucose 120 min following the ingestion of a 75-g sugar water beverage (PPG_{120}) in the EECP group. PPG_{120} is routinely used by physicians to screen for T2D or IGT. In this context, the EECP group, on average, moved from a response that was consistent with T2D to that observed in prediabetes. However, more robust declines in PPG_{120} have been reported following exercise interventions (19, 31).

Angiogeneisis/vasculogenesis and EECP. VEGF is a potent mediator of both angiogenesis and vasculogenesis that is released in response to shear stress and hypoxia. Compression of the EECP cuffs creates several thousand brief, intermittent bouts of shear stress and hypoxia. For example, in a patient with a heart rate of 60 beats/min there are ~3,600 cycles of compression and relaxation, inducing systolic reactive hyperemia in the legs. In the present study, serum levels of VEGF were elevated to 175% of baseline levels after EECP, suggesting a role for angiogenesis/vasculogenesis in the adaptive mechanism. Indeed, we observed significant improvements in capillary density and the capillary to fiber ratio in biopsy sections of the vastus lateralis following 35 sessions of EECP. Although not statistically significant, there was also a trend ($P < 0.10$) for an increase in the number of capillary contacts per muscle fiber following EECP therapy. Increases in capillarity may be of important physiological relevance as decreases in glucose tolerance are associated with decreases in capillarity density (33). In the present study, change in capillary density was significantly correlated with change in C-ISI values ($P = 0.012$) and there was a trend for correlation with change in HOMA-IR values ($P = 0.078$). The observed improvements in capillarity following EECP may improve delivery of insulin and glucose for uptake in nutritive tissues.

Potential mechanisms for improvement in fasting glycemic control and dynamic indexes of glucose tolerance: evidence for the nitric oxide pathway? Given the increasing evidence that NO is an important contributor to glucose homeostasis in AGT, EECP-mediated improvements in NO bioavailability may contribute to the observed improvements in glucose handling.

Indeed, in the present study, we observed significant improvements in plasma NOx concentrations with concurrent decreases in humoral markers of oxidative stress (8-iso-$PGF_{2\alpha}$) and competitive inhibition of NOS (ADMA). Change in ADMA concentration was significantly correlated with change in HOMA-IR and C-ISI values ($P = 0.018$ and 0.024, respectively) Furthermore, change in 8-iso-$PGF_{2\alpha}$ concentration was significantly correlated with change in HOMA-IR values ($P = 0.023$), which may provide evidence for NO-mediated glucose handling. Although we hypothesized that NO-mediated glucose uptake may be realized through alterations in skeletal muscle AMPK signaling, several other mechanisms exist by which NO may mediate glucose uptake. Similar to exercise, repetitive bouts of EECP-induced shear stress in the vasculature may improve insulin-mediated NO production and endothelium dependent dilation in the resistance arteries. Although not measured in the present study, increasing the delivery of substrates to the muscle microvasculature may facilitate transfer to the interstitial space and enhance metabolic action (38). In skeletal muscle, improvements in NO bioavailability may stimulate glucose uptake through a cGMP-dependent pathway that may involve cyclic GMP-dependent kinase/protein kinase G (PKG) activation (39). NO can also directly activate G protein α-subunits, specifically the proto-oncogene p21ras for glucose transport, which increases glucose uptake through nuclear factor κB (NFκB) signaling (21).

It is important to note that although we did not observe any changes in the Akt, AMPK, and TBC1D4 skeletal muscle cell signaling pathways, we were only able to evaluate one time point. In the present study, muscle biopsies were performed at ~48 h following the last session of EECP therapy in an effort to capture a chronic effect of 35 sessions of EECP therapy in subjects with AGT. Transient changes in signaling pathways could occur acutely with each bout of EECP, similar to the effects observed with a bout of exercise. Therefore, it is possible that we were able to capture increases in total protein content but not necessarily the signal(s) responsible. For example, increased NO bioavailability potentiates NO-mediated and AMPK-dependent increases in peroxisome proliferator-activated receptor-γ coactivator 1α (PGC-1α) transcription and ultimately GLUT-4 protein expression. Furthermore, p38MAPK activity, which can also be increased through AMPK and NO-dependent signaling, can increase PGC-1α transcription through interaction with the MEF-2, CREB, and ATF-2 transcription factors. Although we did not examine p38 MAPK activity or PGC-1α expression, we did observe a 47% increase in GLUT-4 protein expression following 35 sessions of EECP in subjects with AGT. However, change in GLUT-4 protein expression only demonstrated a trend for correlation with change in C-ISI values ($P = 0.061$).

Limitations. First, the present study may have been strengthened by the inclusion of a sham intervention to definitively discount a placebo effect. The authors considered using very low cuff inflation pressures as a sham control. However, the effects of sham EECP on skeletal muscle protein expression, a focus of the present study, are largely unknown. Moreover, only objective measurements were employed in the present study, making it unlikely that placebo had a significant impact on the outcomes reported. Second, the study population of the present study was comprised of individuals who had prediabetes (28%) and overt T2D (72%). However, the distribution of pharmacotherapy and prevalence of T2D was similar between the EECP and control groups. Third, although one can speculate on global changes in capillarity and/or protein expression in skeletal muscle, only a site under direct compression was analyzed. Additionally, variation attributable to the fiber type distribution among the samples analyzed could present an additional source of variation, and, in the present study, capillarity was not normalized to fiber type. Despite these limitations, efforts were made to achieve the least heterogeneity among samples as biopsy sections were taken within 1–2 cm of the baseline site and at the same recorded depth for each procedure. Furthermore, an average of 166 ± 13 fibers were analyzed per biopsy sample through the selection of tissue sections possessing little artifact. Finally, NOx is influenced by exogenous sources and is only a gross index of NO formation in vivo. However, all subjects in the present study strictly followed the NIH low nitrate diet guidelines for 48 h prior to their lab visits, so we are confident that plasma NOx levels were influenced minimally.

Conclusions. AGT is associated with several perturbations in normal human physiology, including, but not limited to, endothelial dysfunction, oxidative stress, depressed nitric oxide bioavailability, and progressive declines in capillary density (20, 33). In the present study, we observed significant improvements in fasting glucose and insulin concentrations and significant improvements in glucose tolerance and surrogates of insulin sensitivity. We also observed improvements in measures of arterial function, nitric oxide bioavailability, and capillary density with concurrent decreases in measures of lipid peroxidation and competitive inhibition of NOS. These improvements likely mediate greater delivery of substrates to nutritive tissues (i.e., skeletal muscle) during glycemic challenge. In addition, EECP therapy was associated with increases in skeletal muscle GLUT-4 protein expression, indicating that alteration of skeletal muscle gene expression in compressed tissue may play a role in the adaptive mechanisms observed. This study provides novel evidence for the improvement of vascular function and glycemic control in subjects with AGT following EECP therapy. The multi-factorial nature of AGT makes it likely that more than one of the observed adaptations to EECP therapy contribute to improvements in fasting glucose and insulin concentrations and glucose tolerance. Future studies should be conducted with serial skeletal muscle biopsies during a HEC to accurately describe cellular signaling associated with glucose uptake. Furthermore, the acute effect of EECP and the impact on gene expression profiles and cellular signaling in the skeletal muscle and vasculature should be characterized.

ACKNOWLEDGMENTS

The authors thank all of the subjects for their participation in the study. We also thank all of our colleagues whose expertise was imperative to this research. We are grateful to Jenna J. Harty, William E. Motch, and Blaze D. Emerson for their invaluable work as research assistants.

GRANTS

This research was supported by the Department of Applied Physiology and Kinesiology at the University of Florida.

DISCLOSURES

No conflicts of interest, financial or otherwise, are declared by the authors.

AUTHOR CONTRIBUTIONS

Author contributions: J.S.M., D.T.B., and R.W.B. conception and design of research; J.S.M., D.T.B., and J.M.A. performed experiments; J.S.M. analyzed data; J.S.M., D.T.B., and R.W.B. interpreted results of experiments; J.S.M. prepared figures; J.S.M. drafted manuscript; J.S.M. and R.W.B. edited and revised manuscript; J.S.M., D.T.B., J.M.A., and R.W.B. approved final version of manuscript.

REFERENCES

1. **Andersen P.** Capillary density in skeletal muscle of man. *Acta Physiol Scand* 95: 203–205, 1975.
2. **Arnold-Worner N, Holle R, Rathmann W, Mielck A.** The importance of specialist treatment, treatment satisfaction and diabetes education for the compliance of subjects with type 2 diabetes—results from a population-based survey. *Exp Clin Endocrinol Diabetes* 116: 123–128, 2008.
3. **Arora RR, Chou TM, Jain D, Fleishman B, Crawford L, McKiernan T, Nesto RW.** The multicenter study of enhanced external counterpulsation (MUST-EECP): effect of EECP on exercise-induced myocardial ischemia and anginal episodes. *J Am Coll Cardiol* 33: 1833–1840, 1999.
4. **Bonora E, Targher G, Alberiche M, Bonadonna RC, Saggiani F, Zenere MB, Monauni T, Muggeo M.** Homeostasis model assessment closely mirrors the glucose clamp technique in the assessment of insulin sensitivity: studies in subjects with various degrees of glucose tolerance and insulin sensitivity. *Diabetes Care* 23: 57–63, 2000.
5. **Braith RW, Conti CR, Nichols WW, Choi CY, Khuddus MA, Beck DT, Casey DP.** Enhanced external counterpulsation improves peripheral artery flow-mediated dilation in patients with chronic angina: a randomized sham-controlled study. *Circulation* 122: 1612–1620, 2010.
6. **Braith RW, Magyari PM, Pierce GL, Edwards DG, Hill JA, White LJ, Aranda JM Jr.** Effect of resistance exercise on skeletal muscle myopathy in heart transplant recipients. *Am J Cardiol* 95: 1192–1198, 2005.
7. **Castaneda C, Layne JE, Munoz-Orians L, Gordon PL, Walsmith J, Foldvari M, Roubenoff R, Tucker KL, Nelson ME.** A randomized controlled trial of resistance exercise training to improve glycemic control in older adults with type 2 diabetes. *Diabetes Care* 25: 2335–2341, 2002.
8. **Centers for Disease Control and Prevention.** *2011 National Diabetes Facts Sheet* (online). http://www.cdc.gov/diabetes/pubs/factsheet11.htm (January 18, 2012).
9. **Ceriello A.** Oxidative stress and glycemic regulation. *Metab Clin Exp* 49: 27–29, 2000.
10. **Cramer JA.** A systematic review of adherence with medications for diabetes. *Diabetes Care* 27: 1218–1224, 2004.
11. **Daví G, Ciabattoni A, Consoli A, Mezetti A, Falco A, Santarone S, Pennese E, Vitacolonna E, Bucciarelli T, Costantini F, Capani F, Patrono C.** In vivo formation of 8-iso-prostaglandin F2a and platlet activation in diabetes mellitus: effects of improved metabolic control and vitamin E suuplementation. *Circulation* 99: 224–229, 1999.
12. **Devlin JT, Hirshman M, Horton ED, Horton ES.** Enhanced peripheral and splanchnic insulin sensitivity in NIDDM men after single bout of exercise. *Diabetes* 36: 434–439, 1987.
13. **Doshi SN, Naka KK, Payne N, Jones CJ, Ashton M, Lewis MJ, Goodfellow J.** Flow-mediated dilatation following wrist and upper arm occlusion in humans: the contribution of nitric oxide. *Clin Sci (Lond)* 101: 629–635, 2001.
14. **Evans WJ, Phinney SD, Young VR.** Suction applied to a muscle biopsy maximizes sample size. *Med Sci Sports Exerc* 14: 101–102, 1982.
15. **Gurovich AB, RW.** Three-dimension blood flow classification scheme better describes NO-mediated arterial vasodilation (Abstract). *Med Sci Sports Exerc* 42: 7, 2011.
16. **Higaki Y, Hirshman MF, Fujii N, Goodyear LJ.** Nitric oxide increases glucose uptake through a mechanism that is distinct from the insulin and contraction pathways in rat skeletal muscle. *Diabetes* 50: 241–247, 2001.
17. **Hughes VA, Fiatarone MA, Fielding RA, Kahn BB, Ferrara CM, Shepherd P, Fisher EC, Wolfe RR, Elahi D, Evans WJ.** Exercise increases muscle GLUT-4 levels and insulin action in subjects with impaired glucose tolerance. *Am J Physiol Endocrinol Metab* 264: E855–E862, 1993.
18. **Katz LD, Glickman MG, Rapoport S, Ferrannini E, DeFronzo RA.** Splanchnic and peripheral disposal of oral glucose in man. *Diabetes* 32: 675–679, 1983.
19. **Kelley DE, Goodpaster BH.** Effects of exercise on glucose homeostasis in Type 2 diabetes mellitus. *Med Sci Sports Exerc* 33: S495–501; discussion S528–499, 2001.
20. **Kingwell BA, Formosa M, Muhlmann M, Bradley SJ, McConell GK.** Nitric oxide synthase inhibition reduces glucose uptake during exercise in individuals with type 2 diabetes more than in control subjects. *Diabetes* 51: 2572–2580, 2002.
21. **Lander HM, Sehajpal PK, Novogrodsky A.** Nitric oxide signaling: a possible role for G proteins. *J Immunol* 151: 7182–7187, 1993.
22. **Lira VA, Soltow QA, Long JH, Betters JL, Sellman JE, Criswell DS.** Nitric oxide increases GLUT4 expression and regulates AMPK signaling in skeletal muscle. *Am J Physiol Endocrinol Metab* 293: E1062–E1068, 2007.
23. **Maritim AC, Sanders RA, Watkins JB III.** Diabetes, oxidative stress, antioxidants: a review. *J Biochem Mol Toxicol* 17: 24–38, 2003.
24. **Masuda D, Nohara R, Hirai T, Kataoka K, Chen LG, Hosokawa R, Inubushi M, Tadamura E, Fujita M, Sasayama S.** Enhanced external counterpulsation improved myocardial perfusion and coronary flow reserve in patients with chronic stable angina; evaluation by (13)N-ammonia positron emission tomography. *Eur Heart J* 22: 1451–1458, 2001.
25. **Matsuda M, DeFronzo RA.** Insulin sensitivity indices obtained from oral glucose tolerance testing: comparison with the euglycemic insulin clamp. *Diabetes Care* 22: 1462–1470, 1999.
26. **Metter EJ, Windham BG, Maggio M, Simonsick EM, Ling SM, Egan JM, Ferrucci L.** Glucose and insulin measurements from the oral glucose tolerance test and mortality prediction. *Diabetes Care* 31: 1026–1030, 2008.
27. **Montuschi P, Barnes PJ, Roberts LJ 2nd.** Isoprostanes: markers and mediators of oxidative stress. *FASEB J* 18: 1791–1800, 2004.
28. **Monzillo LU, Hamdy O.** Evaluation of insulin sensitivity in clinical practice and in research settings. *Nutr Rev* 61: 397–412, 2003.
29. **Osanai T, Saitoh M, Sasaki S, Tomita H, Matsunaga T, Okumura K.** Effect of shear stress on asymmetric dimethylarginine release from vascular endothelial cells. *Hypertension* 42: 985–990, 2003.
30. **Pannala AS, Mani AR, Spencer JP, Skinner V, Bruckdorfer KR, Moore KP, Rice-Evans CA.** The effect of dietary nitrate on salivary, plasma, and urinary nitrate metabolism in humans. *Free Radic Biol Med* 34: 576–584, 2003.
31. **Rogers MA, Yamamoto C, King DS, Hagberg JM, Ehsani AA, Holloszy JO.** Improvement in glucose tolerance after 1 wk of exercise in patients with mild NIDDM. *Diabetes Care* 11: 613–618, 1988.
32. **Sakamoto K, Hirshman MF, Aschenbach WG, Goodyear LJ.** Contraction regulation of Akt in rat skeletal muscle. *J Biol Chem* 277: 11910–11917, 2002.
33. **Solomon TP, Haus JM, Li Y, Kirwan JP.** Progressive hyperglycemia across the glucose tolerance continuum in older obese adults is related to skeletal muscle capillarization and nitric oxide bioavailability. *J Clin Endocrinol Metab* 96: 1377–1384, 2011.
34. **Sydow K, Munzel T.** ADMA and oxidative stress. *Atherosclerosis* 4: 41–51, 2003.
35. **Szuba A, Podgorski M.** Asymmetric dimethylarginine (ADMA) a novel cardiovascular risk factor—evidence from epidemiological and prospective clinical trials. *Pharmacol Rep* 58, *Suppl*: 16–20, 2006.
36. **Urano H, Ikeda H, Ueno T, Matsumoto T, Murohara T, Imaizumi T.** Enhanced external counterpulsation improves exercise tolerance, reduces exercise-induced myocardial ischemia and improves left ventricular diastolic filling in patients with coronary artery disease. *J Am Coll Cardiol* 37: 93–99, 2001.
37. **Uusitupa MI.** Early lifestyle intervention in patients with non-insulin-dependent diabetes mellitus and impaired glucose tolerance. *Ann Med* 28: 445–449, 1996.
38. **Vincent MA, Clerk LH, Lindner JR, Klibanov AL, Clark MG, Rattigan S, Barrett EJ.** Microvascular recruitment is an early insulin effect that regulates skeletal muscle glucose uptake in vivo. *Diabetes* 53: 1418–1423, 2004.
39. **Young ME, Leighton B.** Fuel oxidation in skeletal muscle is increased by nitric oxide/cGMP—evidence for involvement of cGMP-dependent protein kinase. *FEBS Lett* 424: 79–83, 1998.
40. **Zhang Y, He X, Chen X, Ma H, Liu D, Luo J, Du Z, Jin Y, Xiong Y, He J, Fang D, Wang K, Lawson WE, Hui JC, Zheng Z, Wu G.** Enhanced external counterpulsation inhibits intimal hyperplasia by modifying shear stress responsive gene expression in hypercholesterolemic pigs. *Circulation* 116: 526–534, 2007.